SOLUTION OF TEAM BENCHMARK PROBLEM #13
(3-D NONLINEAR MAGNETOSTATIC MODEL)

O. Biro, Ch. Magele, G. Vrisk
Graz University of Technology, Kopernikusgasse 24, A-8010 Graz, Austria

Abstract - **Problem No. 13 of the TEAM Workshops is solved by two scalar potential and one vector potential finite-element formulations. The results obtained by the different scalar potential methods are identical and their agreement with those yielded by the vector potential approach and also with measurement data is satisfactory.**

Problem definition

This three-dimensional, non-linear, magnetostatic problem has been proposed by Prof. T. Nakata and K. Fujiwara as a benchmark problem for the TEAM Workshops. For convenience, its definition is repeated here [1,6].

The model is shown in Fig. 1. An exciting coil is placed between two steel channels shifted as shown and a steel plate is inserted between the channels. The material of the steel is nonlinear, the magnetization curve is shown in Fig. 2. The curve can be approximated for high flux densities ($B > 1.8\ T$) as

$$\left.\begin{array}{ll} B = \mu_0 H + (aH^2 + bH + c) & (1.8T \le B \le 2.22T) \\ B = \mu_0 H + M_S & (B \ge 2.22T) \end{array}\right\} \qquad (1)$$

where μ_0 is the permeability of free space. The constants a, b and c are -2.822x10^{-10},2.529x10^{-5} and 1.591, respectively. M_S is the saturation magnetization (2.16 T) of the steel. The coil is excited by a d.c. current. The total current is 1000 AT in one case and 3000 AT in the other. Presently the problem is only open for the 1000 AT case.

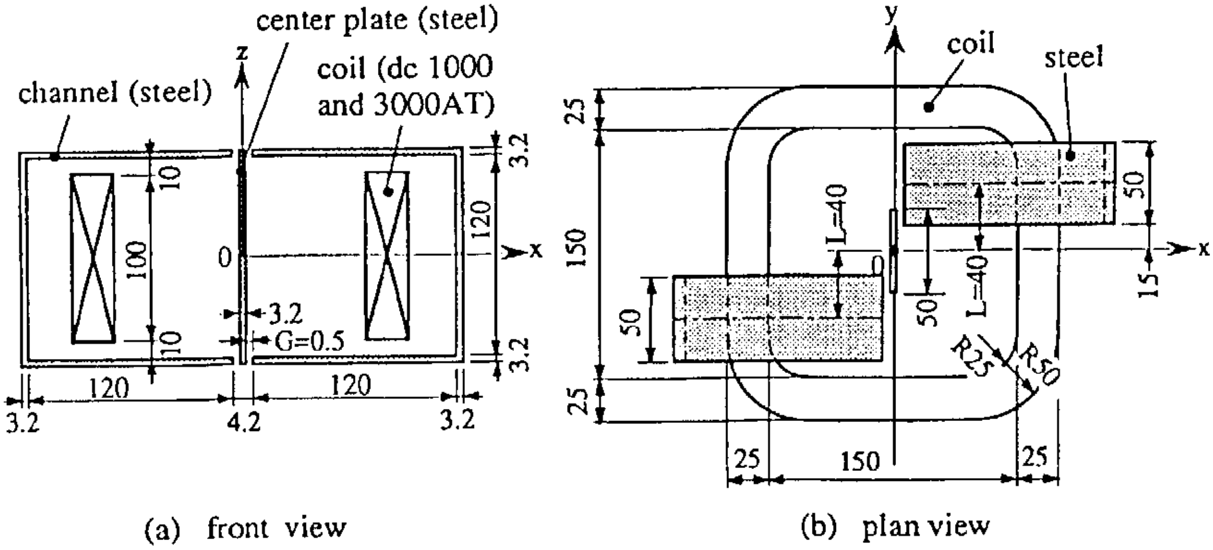

Fig. 1: 3-D nonlinear magnetostatic model (dimensions in mm)

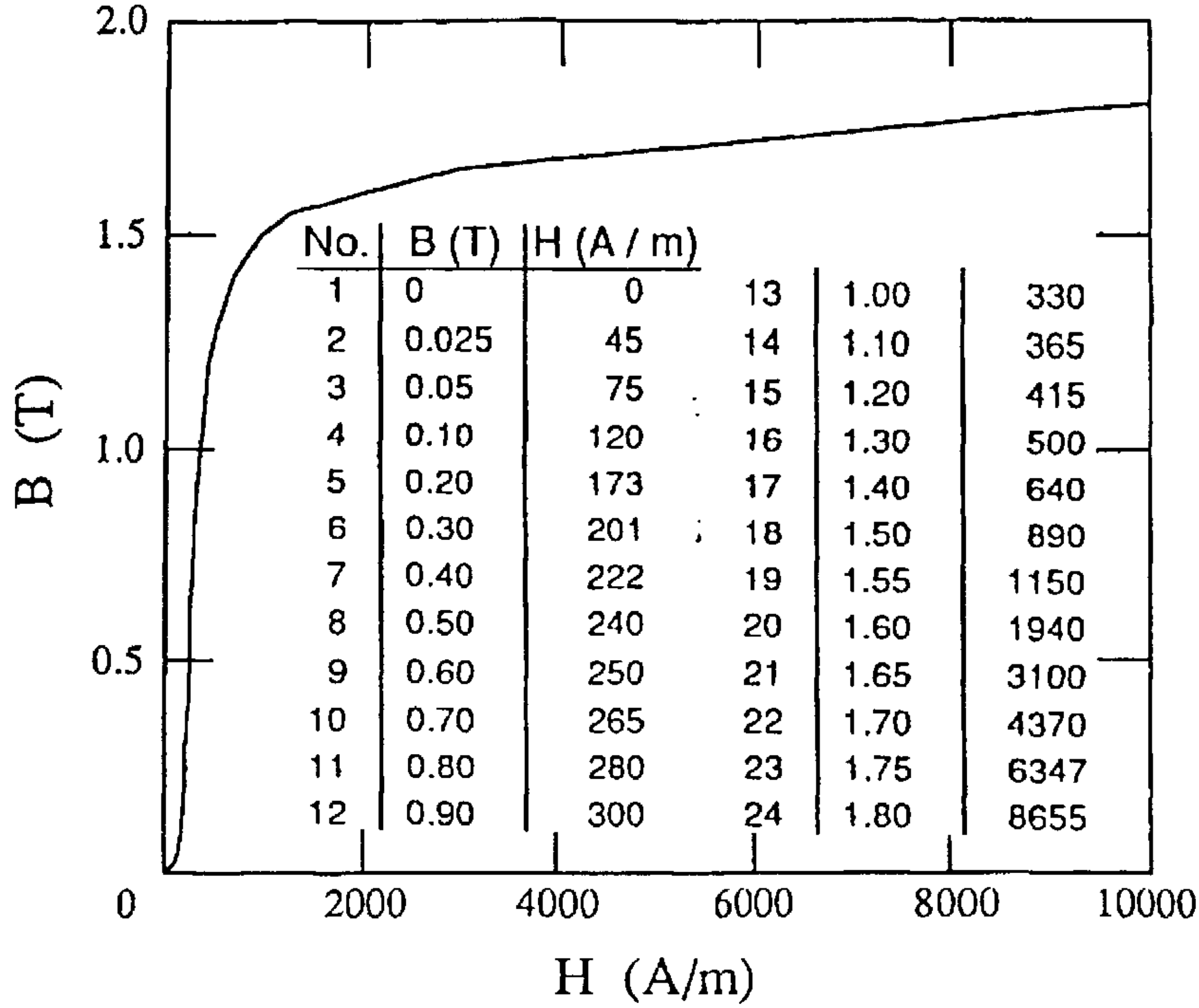

No.	B (T)	H (A / m)	No.	B (T)	H (A / m)
1	0	0	13	1.00	330
2	0.025	45	14	1.10	365
3	0.05	75	15	1.20	415
4	0.10	120	16	1.30	500
5	0.20	173	17	1.40	640
6	0.30	201	18	1.50	890
7	0.40	222	19	1.55	1150
8	0.50	240	20	1.60	1940
9	0.60	250	21	1.65	3100
10	0.70	265	22	1.70	4370
11	0.80	280	23	1.75	6347
12	0.90	300	24	1.80	8655

Fig. 2: B-H curve of steel

It is required to obtain the average flux densities at several locations in the channels and in the center plate as well as along a line and at some specified points in air (see e.g. Tables 1.1 to 1.3)

The problem has been solved with the program package IGTEMAG3D of the Institute for Fundamentals and Theory in Electrical Engineering of the Graz University of Technology. Three solutions have been obtained, two by formulations using a magnetic scalar potential and one by employing a magnetic vector potential. The finite element meshes have been selected so that the number of degrees of freedom is about 200,000.

Φ–Ψ formulation

This is the well known formulation in terms of a reduced and a total magnetic scalar potential [2]. The magnetic field intensity in the free space region is written as

$$\mathbf{H} = \mathbf{H}_s - \nabla\Phi \tag{2}$$

using the reduced scalar potential Φ and the source field $\mathbf{H}_S$ due to the coil in free space computed by Biot-Savart integration. In the iron regions, the magnetic field intensity can be derived from the total scalar potential Ψ:

$$\mathbf{H} = -\nabla\Psi. \tag{3}$$

The two potentials are linked at the interface using the continuity condition of the tangential component of **H**:

$$\Phi = \Psi - \int \mathbf{H}_{St} \cdot \mathbf{ds}. \tag{4}$$

The average flux density values in the three sections of the channel, along the specified line in the air and at the specified points are shown in Tables 1.1, 1.2 and 1.3. Some further information concerning the computation is summarized in Table 1.4.

T-Φ formulation

This is the well known T-Ω method [3] where the magnetic field intensity is written as

$$\mathbf{H} = \mathbf{T} - \nabla\Phi. \tag{5}$$

The function **T** is selected to satisfy

$$\nabla \times \mathbf{T} = \mathbf{J}. \tag{6}$$

In the present calculation **T** was chosen to have a single axial component assuming a constant value in the air core of the racetrack coil, linearly decreasing to zero within the windings and zero outside the coil. To avoid cancellation errors, **T** was represented with the aid of edge elements by computing its integral along each edge in the finite element mesh [4].

The average flux density values in the three sections of the channel, along the specified line in the air and at the specified points are shown in Tables 2.1, 2.2 and 2.3. Some further information concerning the computation is summarized in Table 2.4.

The results are practically identical to those obtained by the Φ–Ψ formulation. The computation time is somewhat lower since no Biot-Savart integration is necessary. In the conjugate gradient iterations, it suffices to use a convergence criterion of 10^{-7} instead of 10^{-12} with respect to the right hand side vector in order to attain the same precision in the solution.

No.	coordinates (mm)			B(T)
	x	y	z	
1			0.0	1.420
2			10.0	1.406
3			20.0	1.373
4	0.0<x<1.6	-25.0<y<25.0	30.0	1.317
5			40.0	1.232
6			50.0	1.072
7			60.0	0.608
8	2.1			0.320
9	10.0			0.594
10	20.0			0.678
11	30.0			0.735
12	40.0			0.785
13	50.0	15.0<y<65.0	60.0<z<63.2	0.827
14	60.0			0.865
15	80.0			0.931
15	100.0			0.974
17	110.0			0.980
18	122.1			0.950
19			60.0	0.885
20			50.0	0.988
21			40.0	0.994
22	122.1<x<125.3	15.0<y<65.0	30.0	0.999
23			20.0	1.003
24			10.0	1.006
25			0.0	1.007

Table 1.1: Average flux densities in steel (T) Φ–Ψ formulation

No	coordinates (mm)			B(T)
	x	y	z	
26	10.0			0.0348
27	20.0			0.0209
28	30.0			0.0164
29	40.0			0.0143
30	50.0			0.0130
31	60.0	20.0	55.0	0.0120
32	70.0			0.0109
33	80.0			0.00876
34	90.0			0.00569
35	100.0			0.00287
36	110.0			0.00140

Table 1.2: Flux density in air (T) Φ–Ψ formulation

No	coordinates (mm)			B(T)
	x	y	z	
37	2.2	15.1	60.1	1.797
38	2.0	14.9	50.9	0.0287
39	1.5	0.0	55.0	0.517
40	1.5	0.0	25.0	1.349

Table 1.3: Flux densities in special points (T) Φ–Ψ formulation

No	Item	Specification
1	Code name	IGTEMAG3D
2	Formulation	FEM (Finite Element Method)
3	Governing equations	$\nabla\cdot(\mu\nabla\Phi)=\nabla\cdot(\mu\mathbf{H}_s)$ $\nabla\cdot(\mu\nabla\Psi)=0$
4	Solution variables	Φ, Ψ
5	Gauge condition	not applicable
6	Fraction of geometry	1/4
7	Technique for non-linear problem	Incremental method
	Convergence criterion	mean ($\Delta\mu_r/\mu_r$) < 1% over all Gaussian points max ($\Delta\mu_r/\mu_r$) < 5% over all Gaussian points
8	Approximation method of B-H curve	straight lines
9	Technique for open boundary problem	truncation
10	Calculation method of magnetic field produced by exciting current	Biot-Savart law (analytical) Biot-Savart law (numerical)
11	Property of coefficient matrix of linear equations	symmetric, sparse
12	Solution method for linear equations	ICCG
	Convergence criterion for iteration method	$\|Ax+b\|^2/\|b\|^2 < 10^{-12}$
13	Element type	hexahedron nodal element (20 nodes)
14	Number of elements	48,384
15	Number of nodes	206,991
16	Number of unknowns	182,517
17	Computer	name: DECstation 5000-240 speed: 40 MIPS main memory: 264 MB precision of data: 64 bits CPU time total: 17,899 s

Table 1.4: Computational data, Φ–Ψ formulation

No.	coordinates (mm)			B(T)
	x	y	z	
1			0.0	1.419
2			10.0	1.406
3			20.0	1.377
4	$0.0<x<1.6$	$-25.0<y<25.0$	30.0	1.322
5			40.0	1.237
6			50.0	1.076
7			60.0	0.610
8	2.1			0.320
9	10.0			0.594
10	20.0			0.678
11	30.0			0.736
12	40.0			0.786
13	50.0	$15.0<y<65.0$	$60.0<z<63.2$	0.828
14	60.0			0.866
15	80.0			0.931
15	100.0			0.974
17	110.0			0.980
18	122.1			0.950
19			60.0	0.886
20			50.0	0.988
21			40.0	0.994
22	$122.1<x<125.3$	$15.0<y<65.0$	30.0	0.999
23			20.0	1.003
24			10.0	1.006
25			0.0	1.007

Table 2.1: Average flux densities in steel (T)
T-Φ formulation

No	coordinates (mm)			B(T)
	x	y	z	
26	10.0			0.0348
27	20.0			0.0209
28	30.0			0.0163
29	40.0			0.0142
30	50.0			0.0130
31	60.0	20.0	55.0	0.0120
32	70.0			0.0108
33	80.0			0.00873
34	90.0			0.00568
35	100.0			0.00296
36	110.0			0.00141

Table 2.2: Flux density in air (T)
T-Φ formulation

No	coordinates (mm)			B(T)
	x	y	z	
37	2.2	15.1	60.1	1.797
38	2.0	14.9	50.9	0.0287
39	1.5	0.0	55.0	0.517
40	1.5	0.0	25.0	1.349

Table 2.3: Flux densities in special points (T)
T-Φ formulation

No	Item	Specification
1	Code name	IGTEMAG3D
2	Formulation	FEM (Finite Element Method)
3	Governing equations	$\nabla \cdot (\mu \nabla \Phi) = \nabla \cdot (\mu \mathbf{T})$ **T** represented by edge elements
4	Solution variables	Φ
5	Gauge condition	not applicable
6	Fraction of geometry	1/4
7	Technique for non-linear problem	Incremental method
	Convergence criterion	mean ($\Delta\mu_r / \mu_r$) < 1% over all Gaussian points max ($\Delta\mu_r / \mu_r$) < 5% over all Gaussian points
8	Approximation method of B-H curve	straight lines
9	Technique for open boundary problem	truncation
10	Calculation method of magnetic field produced by exciting current	taking into account exciting current in governing equations directly
11	Property of coefficient matrix of linear equations	symmetric, sparse
12	Solution method for linear equations	ICCG
	Convergence criterion for iteration method	$\|Ax+b\|^2 / \|b\|^2 < 10^{-7}$
13	Element type	hexahedron nodal element (20 nodes) edge element (36 edges)
14	Number of elements	48,384
15	Number of nodes	206,991
16	Number of unknowns	182,517
17	Computer	name: DECstation 5000-240 speed: 40 MIPS main memory: 264 MB precision of data: 64 bits CPU time total: 13,907 s

Table 2.4: Computational data, **T-Φ** formulation

A-edge formulation

This is a vector potential formulation without a gauge condition, using edge elements to represent **A** [5]. The magnetic flux density is written as

$$\mathbf{B} = \nabla \times \mathbf{A} \tag{7}$$

and the vector potential satisfies the differential equation

$$\nabla \times \left(\nu \nabla \times \mathbf{A} \right) = \mathbf{J} \ . \tag{8}$$

The vector potential is approximated with the aid of edge elements and, in order to make the current density exactly divergence free, it is written in the form (6) with the same function **T** represented by edge elements used as in the **T-Φ** formulation.

The average flux density values in the three sections of the channel, along the specified line in the air and at the specified points are shown in Tables 3.1, 3.2 and 3.3. Some further information concerning the computation is summarized in Table 3.4.

No.	coordinates (mm)			B(T)
	x	y	z	
1			0.0	1.344
2			10.0	1.333
3			20.0	1.299
4	$0.0<x<1.6$	$-25.0<y<25.0$	30.0	1.241
5			40.0	1.152
6			50.0	1.015
7			60.0	0.677
8	2.1			0.270
9	10.0			0.556
10	20.0			0.640
11	30.0			0.700
12	40.0			0.749
13	50.0	$15.0<y<65.0$	$60.0<z<63.2$	0.792
14	60.0			0.830
15	80.0			0.895
15	100.0			0.939
17	110.0			0.945
18	122.1			0.950
19			60.0	0.951
20			50.0	0.954
21			40.0	0.959
22	$122.1<x<125.3$	$15.0<y<65.0$	30.0	0.964
23			20.0	0.968
24			10.0	0.971
25			0.0	0.972

Table 3.1: Average flux densities in steel (T)
A-edge formulation

No	coordinates (mm)			B(T)
	x	y	z	
26	10.0			0.0344
27	20.0			0.0202
28	30.0			0.0162
29	40.0			0.0143
30	50.0			0.0130
31	60.0	20.0	55.0	0.0121
32	70.0			0.0108
33	80.0			0.00872
34	90.0			0.00573
35	100.0			0.00285
36	110.0			0.00144

Table 3.2: Flux density in air (T)
A-edge formulation

No	coordinates (mm)			B(T)
	x	y	z	
37	2.2	15.1	60.1	1.524
38	2.0	14.9	50.9	0.0339
39	1.5	0.0	55.0	0.467
40	1.5	0.0	25.0	1.267

Table 3.3: Flux densities in special points (T)
A-edge formulation

No	Item	Specification
1	Code name	IGTEMAG3D
2	Formulation	FEM (Finite Element Method)
3	Governing equations	$\nabla \times (\nu \nabla \times \mathbf{A}) = \mathbf{J}$
4	Solution variables	$\mathbf{A}$
5	Gauge condition	not imposed
6	Fraction of geometry	1/4
7	Technique for non-linear problem	Incremental method
	Convergence criterion	mean ($\Delta\mu_r / \mu_r$) $<$ 1% over all Gaussian points max ($\Delta\mu_r / \mu_r$) $<$ 5% over all Gaussian points
8	Approximation method of B-H curve	straight lines
9	Technique for open boundary problem	truncation
10	Calculation method of magnetic field produced by exciting current	taking into account exciting current in governing equations directly
11	Property of coefficient matrix of linear equations	symmetric, sparse
12	Solution method for linear equations	ICCG
	Convergence criterion for iteration method	$\|Ax+b\|^2/\|b\|^2 < 10^{-7}$
13	Element type	hexahedron edge element (36 edges)
14	Number of elements	19,200
15	Number of nodes	84,083
16	Number of unknowns	225,728
17	Computer	name: DECstation 5000-240 speed: 40 MIPS main memory: 264 MB precision of data: 64 bits CPU time total: 50,412 s

Table 3.4: Computational data, **A**-edge formulation

Results

The computed average flux densities in the steel channels and the flux density in the air are compared in Figs. 3 to 6 with the measured results [6]. Since the two scalar potential methods yield practically identical results, only a single curve is shown for this case in each plot. It seems that the values obtained by the vector potential formulation are somewhat nearer to the measurements in the steel but the deviation between the scalar potential and measured results is much less than it was reported in previous workshops for meshes with lower degrees of refinement [7-10].

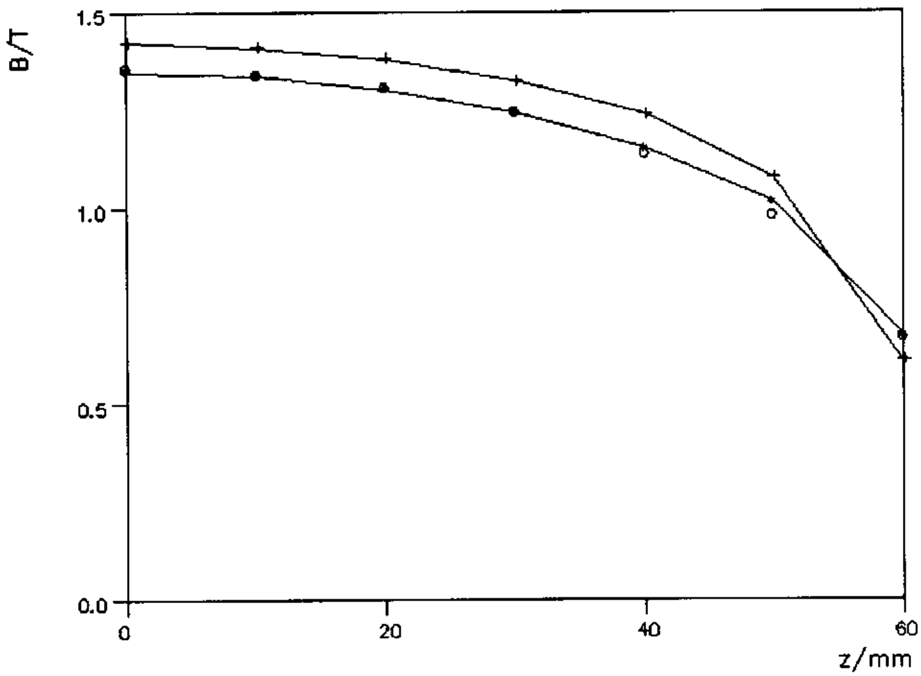

Fig. 3: Average flux density against z , 0 < x < 1.6 mm, -25 < y < 25 mm
o o o o: measurement, —+—+—: scalar potential , —*—*—: vector potential

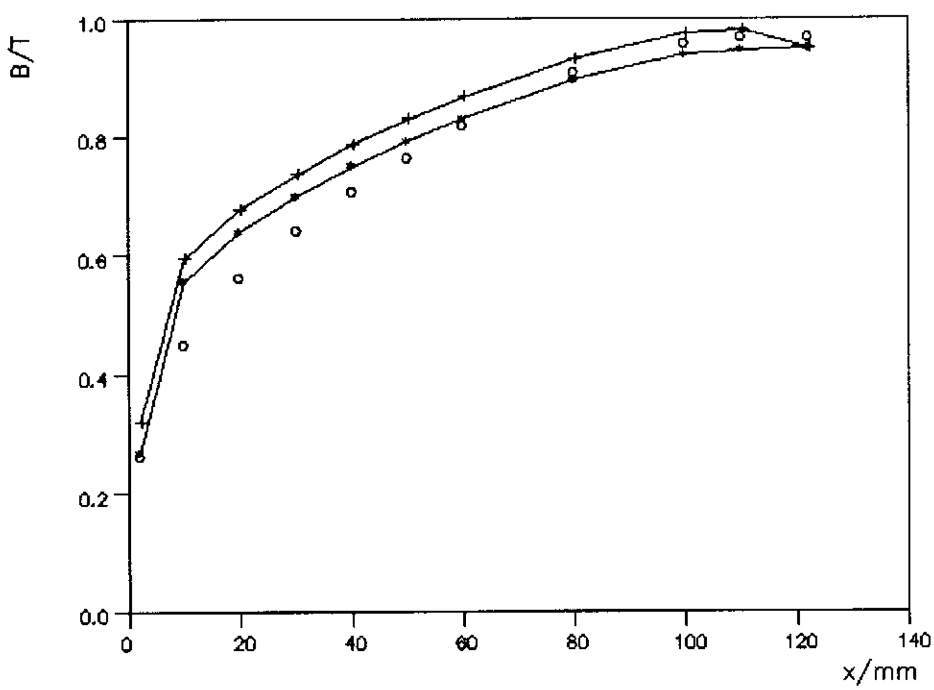

Fig. 4: Average flux density against x, 15 < y < 65 mm, 60 < z < 63.2 mm
o o o o: measurement, —+—+—: scalar potential , —*—*—: vector potential

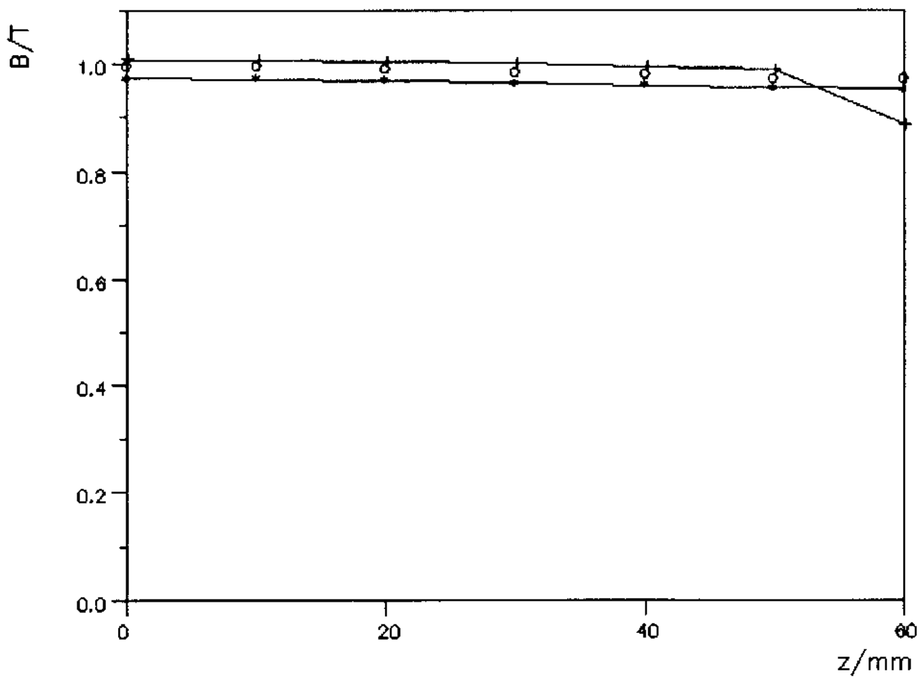

Fig. 5: Average flux density against z, 122.1 < x < 125.3 mm, 15 < y < 65 mm
o o o o: measurement, —+—+—: scalar potential , —*—*—: vector potential

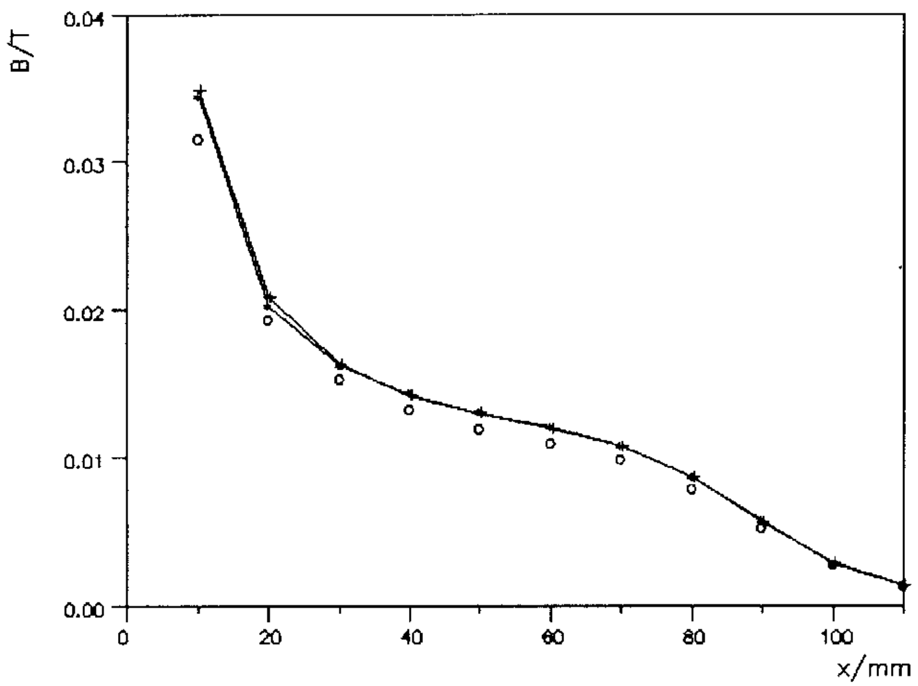

Fig. 6: Flux density against x along the line y = 20 mm, z = 55 mm
o o o o: measurement, —+—+—: scalar potential , —*—*—: vector potential

References

[1] T. Nakata and K. Fujiwara, "Summary of results for benchmark problem 13 (3-d nonlinear magnetostatic model)", in R. Albanese, E. Coccorese, Y. Crutzen and P. Molfino (ed.), *Proc., Third International TEAM Workshop,* Sorrento, Italy, 12-13 July 1991, pp. 223-249

[2] J. Simkin and C. W. Trowbridge, "On the use of the total scalar potential in the numerical solution of field problems in electromagnetics", *Int. J. Numer. Meth. Eng.,* vol. 14, pp. 423-440, 1979.

[3] C. J. Carpenter and E. A. Wyatt, "Efficiency of numerical techniques for computing eddy currents in two and three dimensions", *Proc., COMPUMAG,* Oxford, 31 March to 2 April 1976, pp. 242-250.

[4] O. Biro, K. Preis, G. Vrisk, K.R. Richter and I. Ticar, "Computation of 3-D magnetostatic fields using a reduced scalar potential", *Fifth Biennial IEEE CEFC,* Claremont, CA, August 3-5, 1992. To be published in *IEEE Trans. on Magn.,* vol. 29, March 1993.

[5] A. Kameari, "Calculation of transient 3D eddy current using edge-elements", *IEEE Trans. on Magn.,* vol. 26, pp. 466-469, 1990.

[6] K. Fujiwara, private communication at the TEAM/ACES Workshop, Harvey Mudd College, 6-7 August, 1992.

[7] Y. Crutzen, N.J. Diserens, C.R.I. Emson and D. Rodger (ed.), *Proc., European TEAM Workshop and International Seminar on Electromagnetic Field Analysis,* Oxford, England, 23-25 April 1990, pp. 107-163.

[8] K.R. Richter, W.M. Rucker and O. Biro (ed.), *Proc., 4th International IGTE Symposium and European TEAM Workshop,* Graz, Austria, 10-12 October 1990, pp. 271-291.

[9] L.R. Turner (ed.), *Proc., Toronto TEAM/ACES Workshop,* Ontario Hydro, 25 and 26 October 1990, ANL/FPP/TM-254, pp. 66-78.

[10] R. Albanese, E. Coccorese, Y. Crutzen and P. Molfino (ed.), *Proc., Third International TEAM Workshop,* Sorrento, Italy, 12-13 July 1991, pp. 69-144 and pp. 223-249.